Optical polarization characteristics of semipolar $(30\bar{3}1)$ and $(30\bar{3}\bar{1})$ InGaN/GaN light-emitting diodes

Yuji Zhao,[1,*] Qimin Yan,[2] Daniel Feezell,[2] Kenji Fujito,[3] Chris G. Van de Walle,[2] James S. Speck,[2] Steven P. DenBaars,[1,2] and Shuji Nakamura[1,2]

[1]*Electrical Computer and Engineering Department, University of California, Santa Barbara, California 93106, USA*
[2]*Materials Department, University of California, Santa Barbara, California 93106, USA*
[3]*Optoelectronic Laboratory, Mitsubishi Chemical Corporation, 1000 Higashi-Mamiana, Ushiku, Ibaraki 300-1295, Japan*
[*]*yujizhao@engineering.ucsb.edu*

Abstract: Linear polarized electroluminescence was investigated for semipolar $(30\bar{3}1)$ and $(30\bar{3}\bar{1})$ InGaN light-emitting diodes (LEDs) with various indium compositions. A high degree of optical polarization was observed for devices on both planes, ranging from 0.37 at 438 nm to 0.79 at 519 nm. The extracted valence band energy separation was consistent with the optical polarization ratios. The effect of anisotropic strain on the valance band structure was studied using **k·p** method for the above two planes. The theoretical calculations are consistent with the experimental results.

OCIS codes: (230.3670) Light-emitting diodes; (230.5440) Polarization-selective devices.

References and links

1. S. Nakamura, G. Fasol, and S. J. Pearton, *The Blue Laser Diode: The Complete Story*, 2nd ed. (Springer, 2000).
2. P. Waltereit, O. Brandt, A. Trampert, H. T. Grahn, J. Menniger, M. Ramsteiner, M. Reiche, and K. H. Ploog, "Nitride semiconductors free of electrostatic fields for efficient white light-emitting diodes," Nature **406**(6798), 865–868 (2000).
3. F. Bernardini and V. Fiorentini, "Spontaneous versus piezoelectric polarization in III-V nitrides: conceptual aspects and practical consequences," Phys. Status Solidi B **216**(1), 391–398 (1999).
4. Y. Zhao, J. Sonoda, I. Koslow, C. C. Pan, H. Ohta, J. S. Ha, S. P. Denbaars, and S. Nakamura, "Optimization of devices structures for bright blue semipolar $(10\bar{1}\bar{1})$ light emitting diodes via metalorganic chemical vapor deposition, " Jpn. J. Appl. Phys. **49**, 070206 (2010).
5. Y. Zhao, J. Sonoda, C. C. Pan, S. Brinkley, I. Koslow, K. Fujito, H. Ohta, S. P. DenBaars, and S. Nakamura, "30-mW-class high-power and high-efficiency blue semipolar $(10\bar{1}\bar{1})$ InGaN/GaN light-emitting diodes obtained by backside roughening technique, " Appl. Phys. Express **3**(10), 102101 (2010).
6. Y. Zhao, S. Tanaka, C. C. Pan, K. Fujito, D. Feezell, J. S. Speck, S. P. DenBaars, and S. Nakamura, "High-power blue-violet semipolar $(20\bar{2}\bar{1})$ InGaN/GaN light-emitting diodes with low efficiency droop up at 200A /cm^2," Appl. Phys. Express **4**, 082104 (2011).
7. Y. Zhao, Q. Yan, C. Y. Huang, S. C. Huang, P. S. Hu, S. Tanaka, C. C. Pan, Y. Kawaguchi, K. Fujito, C. G. Van de Walle, J. S. Speck, S. P. DenBaars, S. Nakamura, and D. Feezell, "Indium incorporation and emission properties of nonpolar and semipolar InGaN quantum wells," Appl. Phys. Lett. **100**(20), 201108 (2012).
8. C. C. Pan, S. Tanaka, F. Wu, Y. Zhao, J. S. Speck, S. Nakamura, S. P. DenBaars, and D. Feezell, "High-power, low-efficiency-droop semipolar $(20\bar{2}\bar{1})$ single-quantum-well blue light-emitting diodes, " Appl. Phys. Express **5**(6), 062103 (2012).
9. N. F. Gardner, J. C. Kim, J. J. Wierer, Y. C. Shen, and M. R. Krames, "Polarization anisotropy in the electroluminescence of *m*-plane InGaN-GaN multiple-quantum-well light-emitting diodes," Appl. Phys. Lett. **86**(11), 111101 (2005).
10. L. Schade, U. T. Schwarz, T. Wernicke, J. Rass, S. Ploch, M. Weyers, and M. Kneissl, "On the optical polarization properties of semipolar InGaN quantum wells," Appl. Phys. Lett. **99**(5), 051103 (2011).
11. A. E. Romanov, T. J. Baker, S. Nakamura, and J. S. Speck, "Strain-induced polarization in wurtzite III-nitride semipolar layers," J. Appl. Phys. **100**, 023522 (2006).

#174640 - $15.00 USD Received 20 Aug 2012; revised 25 Oct 2012; accepted 25 Oct 2012; published 4 Dec 2012

12. M. Kubota, K. Okamoto, T. Tanaka, and H. Ohta, "Temperature dependence of polarized photoluminescence from nonpolar *m*-plane InGaN multiple quantum wells for blue laser diodes," Appl. Phys. Lett. **92**(1), 011920 (2008).
13. S. You, T. Detchprohm, M. Zhu, W. Hou, E. A. Preble, D. Hanser, T. Paskova, and C. Wetzel, "Highly polarized green light-emitting diode in *m*-axis GaInN/GaN," Appl. Phys. Express **3**(10), 102103 (2010).
14. S. Brinkley, Y. D. Lin, A. Chakraborty, N. Pfaff, D. Cohen, J. S. Speck, S. Nakamura, and S. P. Denbaars, "Polarized spontaneous emission from blue-green *m*-plane GaN-based light emitting diodes," Appl. Phys. Lett. **98**(1), 011110 (2011).
15. F. Wu, Y. D. Lin, A. Chakraborty, H. Ohta, S. P. DenBaars, S. Nakamura, and J. S. Speck, "Stacking fault formation in the long wavelength InGaN/GaN multiple quantum wells grown on *m*-plane GaN," Appl. Phys. Lett. **96**(23), 231912 (2010).
16. Y. Enya, Y. Yoshizumi, T. Kyono, K. Akita, M. Ueno, M. Adachi, T. Sumitomo, S. Tokuyama, T. Ikegami, K. Katayama, and T. Nakamura, "531 green lasing of InGaN based laser diodes on semi-polar $\{20\bar{2}1\}$ free-standing GaN substrates, " Appl. Phys. Express **2**, 082101 (2009).
17. T. Kyono, Y. Yoshizumi, Y. Enya, M. Adachi, S. Tokuyama, M. Ueno, K. Katayama, and T. Nakamura, "Optical polarization characteristics of InGaN quantum wells for green laser diodes on semi-polar $\{20\bar{2}1\}$ GaN substrates, " Appl. Phys. Express **3**(1), 011003 (2010).
18. S. Yamamoto, Y. Zhao, C. C. Pan, R. B. Chung, K. Fujito, J. Sonoda, S. P. Denbaars, and S. Nakamura, "High-efficiency single-quantum-well green and yellow-green light-emitting diodes on semipolar $(20\bar{2}1)$ GaN substrates, " Appl. Phys. Express **3**(12), 122102 (2010).
19. Y. Zhao, S. Tanaka, Q. Yan, C. Y. Huang, R. B. Chung, C. C. Pan, K. Fujito, D. Feezell, C. G. Van de Walle, J. S. Speck, S. P. DenBaars, and S. Nakamura, "High optical polarization ratio from semipolar $(20\bar{2}\bar{1})$ blue-green InGaN/GaN light-emitting diodes, " Appl. Phys. Lett. **99**(5), 051109 (2011).
20. H. Masui, H. Yamada, K. Iso, H. Hirasawa, N. N. Fellows, J. S. Speck, S. Nakamura, and S. P. DenBaars, "Optical polarization of *m* –plane In-GaN/GaN light-emitting diodes characterized via confocal microscope," Phys. Status Solidi A **205**(5), 1203–1206 (2008).
21. L. Schade, U. T. Schwarz, T. Wernicke, M. Weyers, and M. Kneissl, "Impact of band structure and transition matrix elements on polarization properties of the photoluminescence of semipolar and nonpolar InGaN quantum wells," Phys. Status Solidi B **248**(3), 638–646 (2011).
22. A. Trellakis, T. Zibold, T. Andlauer, S. Birner, R. K. Smith, R. Morschl, and P. Vogl, "The 3D nanometer devices project *nextnano*: concepts, methods, results," J. Comput. Electron. **5**, 285–289 (2006). For the nextnano^3 code, see *http://www.nextnano.de*.
23. C. Roberts, Q. Yan, M. S. Miao, and C. G. Van de Walle, "Confinement effects on valence-subband character abd polarization anisotropy in semipolar $(11\bar{2}2)$ semipolar InGaN/GaN quantum wells, " J. Appl. Phys. **111**, 073113 (2012).
24. M. Ueda, M. Funato, K. Kojima, Y. Kawakami, Y. Narukawa, and T. Mukai, "Polarization switching phenomena in semipolar $In_xGa_{1-x}N$/GaN quantum well active layers," Phys. Rev. B **78**(23), 233303 (2008).
25. S. H. Park and D. Ahn, "Depolarization effects in $(11\bar{2}2)$ -oriented InGaN⁄GaN quantum well structures," Appl. Phys. Lett. **90**(1), 013505 (2007).
26. Q. Yan, P. Rinke, M. Scheffler, and C. G. Van de Walle, "Role of strain in polarization switching in semipolar InGaN/GaN quantum wells," Appl. Phys. Lett. **97**(18), 181102 (2010).
27. A. F. Wright, "Elastic properties of zinc-blende and wurtzite AlN, GaN, and InN," J. Appl. Phys. **82**(6), 2833–2839 (1997).

1. Introduction

Nitride based light-emitting diodes (LEDs) and laser diodes (LDs) have been extensively researched as they promise highly-efficient, cost-effective and environmentally-friendly illumination sources compared to conventional incandescent and fluorescent-based lighting [1]. Conventional GaN-based LEDs and LDs on the "polar" *c*-plane suffers from internal polarization-related electric fields which reduce the quantum well (QW) radiative recombination rate and cause large shifts in emission wavelength with increasing carrier injection [2,3]. To circumvent these polarization effects, device on nonpolar and semipolar orientations have been studied for their potential to realize improved performance including high efficiency, high optical gain, high indium incorporation, and stable emission wavelength [4–8].

In contrast to standard *c*-plane QWs, the unbalanced biaxial stress in the semipolar and nonpolar QWs results in partially polarized spontaneous emission [9]. This optical anisotropy is a consequence of the broken symmetry and associated valance band splitting in the nonpolar and semipolar crystal structure [10]. To describe the strain state, two coordinates system *xyz* and *x'y'z'* are usually defined for the natural and primed coordinate system. For

#174640 - $15.00 USD Received 20 Aug 2012; revised 25 Oct 2012; accepted 25 Oct 2012; published 4 Dec 2012

the natural coordinate system, x is defined along the a-direction and y and z along the m- and c-direction, respectively. For the primed coordinate system, z' is in the direction of template's surface normal, while x' and y' axes are in the template's surface plane with the x' axis coincide with x axis (the rotation axis). The details of the coordinate definitions can be found in Ref [11]. On nonpolar (m-plane) orientation, the reduced symmetry, in comparison to c-plane, and unbalanced plane biaxial stress breaks the x-y plane symmetry and splits the $|x \pm iy\rangle$ state into $|x\rangle$ and $|y\rangle$ state. The emission components polarized along the a- and c-axes involve the highest and second highest valence bands, respectively [12–14]. This polarization property is of great interest to increase light throughput in back lighting systems and also contributes to the anisotropic optical gain in the LDs.

Although high optical polarization ratios have been reported for m-plane devices [12–14], their long wavelength performance has been limited by the generation of basal plane stacking faults in high indium content QWs [15]. Recently, semipolar planes with miscut angles of 10 to 15° toward the c-direction from m-plane have been reported with improved performance in the long wavelength region [16–19]. In this paper, we report a comprehensive study of optical polarization on semipolar $(30\bar{3}1)$ and $(30\bar{3}\bar{1})$ InGaN LEDs (+/–10° from m-plane towards the c-direction) by electroluminescence (EL) measurements. The high optical polarization ratios realized on these two planes are consistent with the calculation results using **k·p** method. Both the experimental data and the simulation result suggest that strain is the dominate factor for the optical polarization properties of both $(30\bar{3}1)$ and $(30\bar{3}\bar{1})$ InGaN QWs.

2. Experiment

LEDs were homoepitaxially grown by conventional metal-organic chemical vapor deposition (MOCVD) on free standing $(30\bar{3}1)$ and $(30\bar{3}\bar{1})$ GaN substrates supplied by Mitsubishi Chemical Corporation. The device structure consists of a 1 μm Si-doped n-type GaN layer, an active region consisting of a 3 nm InGaN single quantum well with 10 nm GaN barriers, a 16 nm Mg-doped $Al_{0.15}Ga_{0.85}N$ electron blocking layer (EBL), and a 60 nm p-type GaN layer. For the LED fabrication, a rectangular mesa pattern (490 × 292 μm^2) was formed by conventional lithography and chlorine-based inductively coupled plasma (ICP) etching after an indium tin oxide (ITO) current spreading layer was deposited by electron beam evaporation. Ti/Al/Ni/Au n-type contacts and Ti/Au pads were deposited by electron beam evaporation and a conventional lift-off process. The peak external quantum efficiencies (EQE) of the semipolar LEDs are in the range of 30 to 40%, which are comparable to the standard commercial c-plane devices.

EL measurements were carried out under direct current (DC) operation at room temperature using a 0.45 numerical aperture 20 × microscope objective designed for collection of polarized light [20]. Black ink with mixed-in carbon black was applied to the bottom and side surfaces of the devices as a photon absorbing element to prevent multiple reflections [14]. The optical polarization ratio (ρ), given by $\rho = (I_{x'} - I_{y'})/(I_{x'} + I_{y'})$, where $I_{x'}$ and $I_{y'}$ are the integrated EL intensities with the polarizer aligned along the x' and y' directions of the sample, respectively. For $(30\bar{3}1)$ samples, the x' is along the $[\bar{1}2\bar{1}0]$ direction while the y' is along the $[\bar{1}0\bar{1}6]$ direction. For $(30\bar{3}\bar{1})$ samples, the x' is along the $[\bar{1}2\bar{1}0]$ direction and the y' is along the $[\bar{1}0\bar{1}\bar{6}]$ direction. The energy separation between the top two valance bands (ΔE), is approximately given by the energy difference between emission peak wavelengths for the two polarizations [21]. The polarization ratios and energy separations for $(30\bar{3}1)$ and $(30\bar{3}\bar{1})$ LEDs are plotted and discussed below. Schematic views of the microscope system used for the polarization measurements, the studied LED structure, and the semipolar crystal planes are shown in Figs. 1(a)-1(c), respectively.

#174640 - $15.00 USD Received 20 Aug 2012; revised 25 Oct 2012; accepted 25 Oct 2012; published 4 Dec 2012

For the theoretical calculations, self-consistent Schrödinger-Poisson simulations were performed on $(30\bar{3}1)$ and $(30\bar{3}\bar{1})$ InGaN/GaN QWs using the nextnano^3 code [22]. The QW of the simulated structures was assumed to be pseudomorphically grown on a GaN substrate and had the identical structure with that of the experimental devices. A small amount of unintentional *n*-type doping with a concentration of 8×10^{16} cm^3 is assumed in both InGaN QW and GaN barriers. By solving the 6 × 6 **k·p** Hamiltonian including strain and polarization fields, the valance band dispersion relationships and the energy separation of the topmost valence bands were obtained for InGaN bulk/QW structures with different indium compositions. The details of simulation structures and parameters can be found in Ref [23].

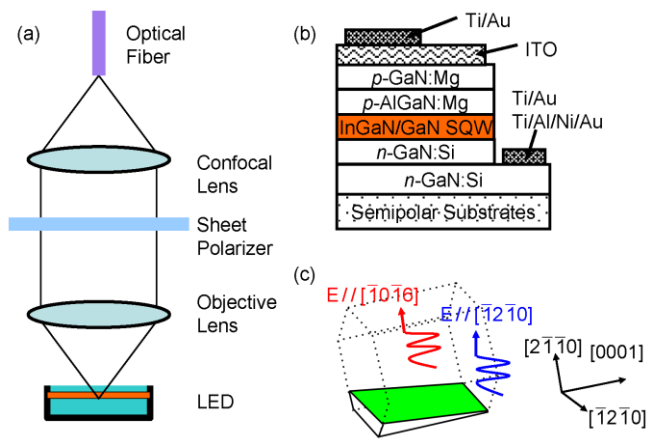

Fig. 1. Schematic views of (a) the microscope system used for the polarization measurements, (b) the studied LED structure, and (c) the semipolar $(30\bar{3}1)$ crystal planes.

3. Results and discussions

Figures 2(a)-2(c) show the EL spectra of $(30\bar{3}\bar{1})$ LEDs at wavelength of 445 nm, 483nm and 509 nm, respectively. The emission component polarized along the $[\bar{1}2\bar{1}0]$ plane is dominant, as indicated by the higher intensity compared to that of the component polarized along the $[\bar{1}0\bar{1}6]$ plane. These results are consistent with those found on semipolar $(20\bar{2}\bar{1})$ and $(20\bar{2}1)$ LEDs, where the light polarized along the projection of *a*-direction are the dominant component [19]. It is reported that for certain semipolar planes (e.g., $(11\bar{2}2)$ plane), the optical polarization switches for QWs with high indium compositions [10,24]. This switching phenomenon was not observed for $(30\bar{3}\bar{1})$ nor $(30\bar{3}1)$ devices. This is consistent with Schade *et al*. as semipolar planes with inclination angles higher than 69.4° are not affected by the polarization switching mechanism [10]. The intensity difference between the two components becomes larger as the wavelength increases, which is in good agreement with the theory. Similar results were obtained for $(30\bar{3}1)$ LEDs from blue to green region (Figs. 2(d)-2(e)).

Figure 3 shows the (a) polarization ratio and (b) ΔE of $(30\bar{3}\bar{1})$ and $(30\bar{3}1)$ LEDs as a function of the peak wavelength of the dominant emission. At comparable wavelength, devices of two planes show almost identical polarization ratio and degrees of band splitting. The values obtained are similar to that of *m*-plane [12–14]. Both the polarization ratios and the ΔE on the two planes show a monotonic increase with wavelength, which in good agreement with theoretical predictions [19]. It is anticipated that by incorporating more indium in the QWs, the unbalanced plane stress increases and thus further splits the valence

#174640 - $15.00 USD Received 20 Aug 2012; revised 25 Oct 2012; accepted 25 Oct 2012; published 4 Dec 2012

bands. It has been theoretically predicted and experimentally verified that a high polarization ratio is preferable for achieving increased optical gain in laser diodes [25]. Devices grown on these semipolar planes exhibit high optical polarization ratios and therefore may facilitate improved LD performance in the green spectral region [16,17]. LEDs with high optical polarization will also contribute to enhance the system power efficiency in the back lighting units [13].

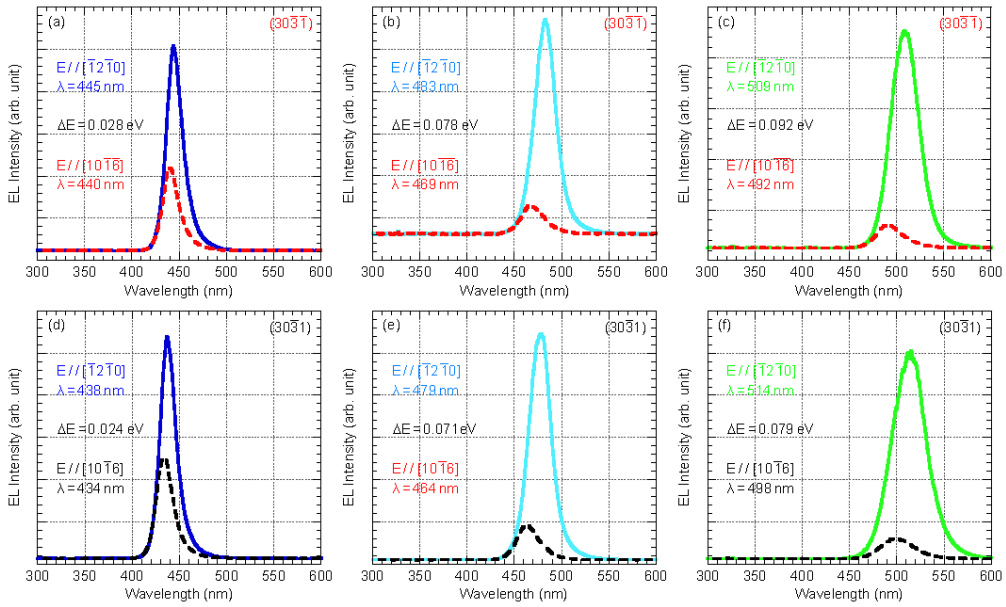

Fig. 2. Electroluminescence spectra of (30$\bar{3}\bar{1}$) InGaN LEDs at a wavelength of (a) 445 nm, (b) 483 nm, and (c) 509 nm, showing increasing polarization ratio and energy separation with increasing wavelength. Similar results were obtained for (30$\bar{3}$1) LEDs at a wavelength of (d) 438 nm, (e) 479 nm, and (f) 514 nm.

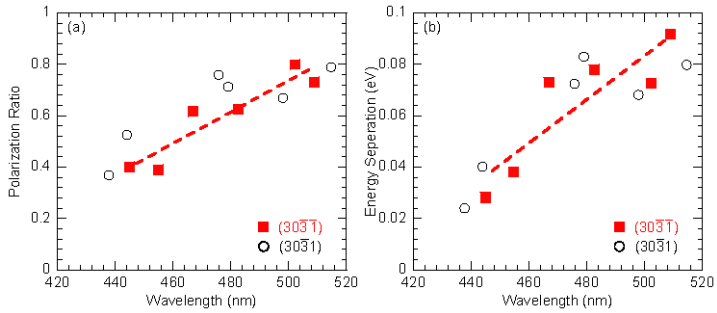

Fig. 3. (a) Optical polarization and (b) energy separation (ΔE) with increasing wavelength for (30$\bar{3}\bar{1}$) and (30$\bar{3}$1) LEDs. Red dash lines are the simulated trend for the experimental data.

It has been theoretically suggested that polarized emission from nonpolar and semipolar InGaN QWs is caused by unbalanced plane stress in the InGaN quantum wells [26]. To investigate the strain conditions and associated subband structures of the semipolar InGaN QW, strain components in the InGaN alloy must be determined. The lattice parameters of an unstrained InGaN alloy can be obtained by the Vegard's law which simply averages over all local distortions: $a_{InGaN} = xa_{InN} + a_{GaN}(1-x)$. The lattice mismatch to the GaN substrate induces composition-dependent compressive in-plane strain. The strain components in and out of the

#174640 - $15.00 USD Received 20 Aug 2012; revised 25 Oct 2012; accepted 25 Oct 2012; published 4 Dec 2012

c-plane, which are needed for the **k·p** approach, can be determined from the lattice mismatch [10]. Figure 4 presents the calculated strain components for semipolar $(30\bar{3}1)$ QWs in the normal *c*-plane coordinate system. The details of the elastic constants used in the calculations can be found in Ref [27]. These pseudomorphic stress conditions lead to anisotropic strain in the *c*-plane ($|\varepsilon_{xx}-\varepsilon_{yy}| \neq 0$), and a large shear-strain component ε_{xz}. For the $(30\bar{3}\bar{1})$ alloy, the magnitudes of strain components are the same as those in the $(30\bar{3}1)$ InGaN alloy, except that the shear-strain component has a negative sign. From our analytical calculations, identical band structures were obtained for both $(30\bar{3}1)$ and $(30\bar{3}\bar{1})$ bulk InGaN alloys strained on GaN substrates, as expected from crystal symmetry.

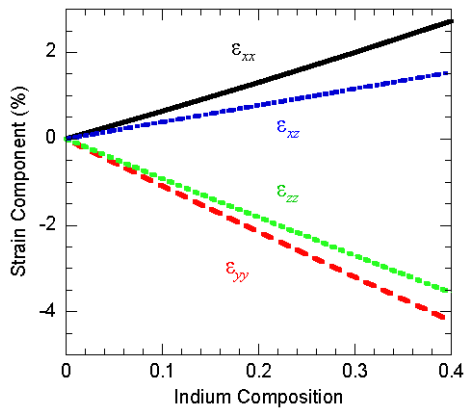

Fig. 4. Strain components in semipolar $(30\bar{3}1)$ InGaN grown on GaN as a function of indium composition: *x*, *y* and *z* refer to the natural coordinate system.

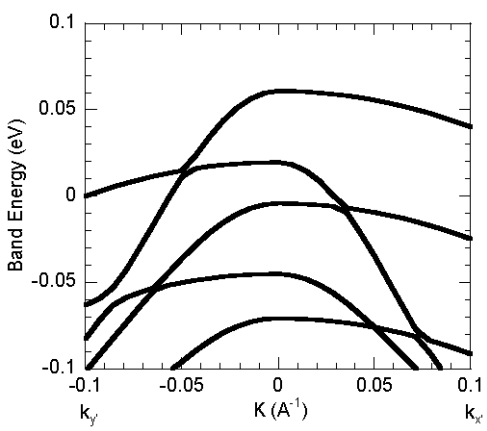

Fig. 5. The calculated valance band dispersion relation for semipolar $(30\bar{3}1)$ InGaN/GaN QW with an indium composition of 20%.

As the optical polarization ratio is measured from the light emitted from InGaN QWs, the quantum-confinement effect has to be taken into account. A typical InGaN QW is only a few nm wide, the confinement effect can thus in principle change the energy separation of the topmost subbands. Figure 5 shows the subband structure of a 3 nm semipolar $(30\bar{3}1)$ $In_{0.2}Ga_{0.8}N$ QW, calculated by using the self-consistent Schrödinger-Poisson simulations. The quantum confinement leads to the formation of several valence subbands in the QW structures. For $(30\bar{3}1)$ and $(30\bar{3}\bar{1})$ QWs, at Γ point, the topmost subband has $|x'\rangle$ -like

#174640 - $15.00 USD Received 20 Aug 2012; revised 25 Oct 2012; accepted 25 Oct 2012; published 4 Dec 2012

character and the second band has $|y'\rangle$-like character. The energy separation (ΔE) is defined as the difference of these two topmost valance subbands at the Γ point. Figure 6 presents the ΔE for both InGaN bulk and QW (3 nm) structures on semipolar $(30\bar{3}1)$ GaN substrates with different indium compositions. The energy separation increases with increasing indium compositions in both bulk material and the QW structures, suggesting that the strain is the dominate factor in determining the degree of energy separations and associated optical polarizations. This is consistent with the experimental data (Fig. 3(b)). The difference between the bulk and QW results is however very small (less than 5 meV), indicating that the quantum-confinement effect on the band separation is not significant.

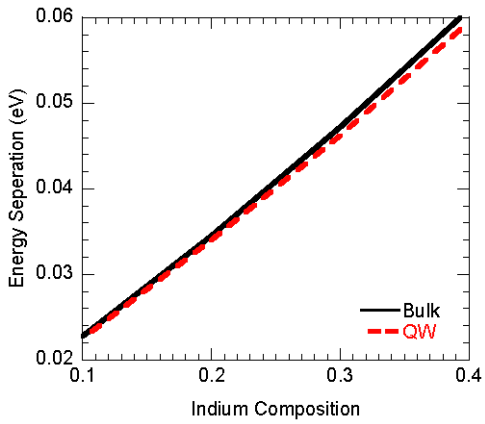

Fig. 6. The calculated energy separation (ΔE) between the top two valance bands at the Γ point $(30\bar{3}1)$ InGaN QW and bulk structures.

4. Conclusion

In summary, we have grown and fabricated LEDs on the semipolar $(30\bar{3}\bar{1})$ and $(30\bar{3}1)$ plane with emission wavelengths ranging from blue to green. These devices have shown high optical polarization ratios and large valance band separations, which may facilitate improved LD performance and reduced power consumption in the back lighting systems. The obtained experiment data are consistent with simulated values obtained by the **k·p** method. The simulation also suggest that strain is the dominate factor for the optical polarization properties of above semipolar QWs, while the quantum-confinement effect is not prominent.

Acknowledgment

The authors acknowledge the support of Solid State Lighting and Energy Center (SSLEC) at UCSB. A portion of this work was done in the UCSB nanofabrication facility, part of the NSF funded NNIN.